Contents

Part A: Single Phase Materials

Part B: Phase Transformations

Part A

Single Phase Materials

Chapter 1

Defects in Quenched and Irradiated Face-Centered Cubic Metals

M. J. WHELAN

I. Introduction

When a metal is quenched from high temperatures or subjected to bombardment by high energy nuclear particles, a large number of point defects in excess of the equilibrium concentration may be trapped in the lattice. In the former case, only vacancies are thought to be produced in appreciable numbers, whereas in the latter case, vacancies and interstitial atoms will be produced in equal numbers in the interior of the metal at collision sites. The changes in physical properties due to the point defects (e.g., electrical resistivity, density, hardness, and plastic properties) and their variation on subsequent annealing have therefore been the subject of much experimental and theoretical investigation in recent years (see the reviews by Cottrell (1), Seitz and Koehler (2), Kinchin and Pease (3), Glen (4), Dienes and Vineyard (5), Cottrell (6)). While much has been learned from such studies concerning activation energies of formation and migration of defects (see references (7–17) for quenching and (18–28) for irradiation effects), the nature and distribution of the defects introduced and the mechanisms of annealing remained speculative in many cases. For example, it was uncertain whether vacancies in quenched metals clustered to form cavities at dislocations (Coulomb and Friedel (29)), dislocation loops (Kuhlmann-Wilsdorf (30)), or jogs at dislocations (Cottrell (6)).

Recently, however, methods of direct observation by transmission electron microscopy have been employed to study a number of problems in quenching and radiation damage. While much remains obscure, many facts of interest have emerged. The object of this paper is to review the electron microscope evidence obtained so far on the microstructure of quenched and irradiated face-centered cubic metals, and to discuss it in the light of evidence obtained from measurement of other physical properties.

II. Defects Produced by Quenching

A. GENERAL

The equilibrium concentration c of vacancies in a metal (the fraction of sites vacant) increases with temperature T according to the equation

$$c = A \exp(-E_f/kT) \tag{1}$$

where A is an entropy factor (taken to be of order unity), E_f is the energy of formation of a vacancy, and k is Boltzmann's constant. In aluminum, for example, $E_f \simeq 0.76$ ev (Bradshaw and Pearson (9)). Taking $k = 0.86 \times 10^{-4}$ ev degree C^{-1}, we find that $c \sim 10^{-4}$ near the melting point and that $c \sim 10^{-13}$ at room temperature. Assuming that all the vacancies are retained in a quench, the vacancy supersaturation at room temperature ($\sim 10^9$) is very large indeed.

Frank (31) and Seitz (32) first suggested that the excess vacancies might precipitate in the form of discs which would subsequently collapse to form loops of dislocation line, as shown schematically in Figure 1(b–d). This idea was developed by Kuhlmann-Wilsdorf (30), who also pointed out certain differences in the properties of the loops in face-centered cubic metals of different stacking fault energy. Figure 2a shows Thompson's notation (33) for denoting slip planes and Burgers vectors in the face-centered cubic structure. The tetrahedron $ABCD$ has edges parallel to the six close-packed $\langle 110 \rangle$ directions and faces parallel to the four close-packed $\{111\}$ planes. The edge length is equal to the length of the Burgers vector $\frac{1}{2}\langle 110 \rangle$ of a whole dislocation. The midpoints of the faces opposite A, B, C, and D are denoted

by α, β, γ, and δ. Imagine that the dislocation loop in Figure 1d lies in the plane BCD of Figure 2a (plane α). If it is formed by removal of part of a B-plane and straight collapse (as shown in Fig. 1d), the Burgers vector of the loop will be $\frac{1}{3}\langle 111\rangle$ or αA. The dislocation is a Frank sessile dislocation, enclosing a region of intrinsic stacking fault (Frank (34)). However, as pointed out by Kuhlmann-Wilsdorf (30), it may be energetically favorable for such a loop to revert to a whole dislocation line by shear of the C-

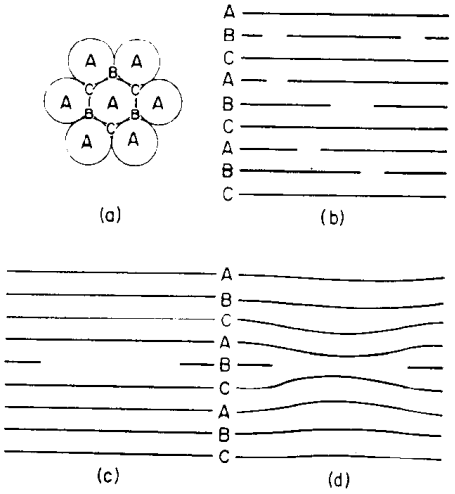

Fig. 1. Schematic diagram illustrating dislocation loop formation by vacancies in a face-centered cubic metal. (a) Stacking sequence (b) random vacancies (c) disc of vacancies (d) collapsed disc with intrinsic stacking fault.

layer bounding the vacancy disc to a B-position, thereby removing the stacking fault. Such a shear is represented by any one of the vectors $B\alpha$, $C\alpha$, $D\alpha$ in Figure 2a, which are Burgers vectors of Shockley partial dislocations glissile in plane α. For example, the reaction $B\alpha + \alpha A \rightarrow BA$ will produce a whole dislocation loop of Burgers vector BA. While the original sessile loop was constrained to lie on α, it will be noted that the whole dislocation loop can glide on the prismatic cylinder containing the loop and the direction of the Burgers vector, and is therefore called a "prismatic" dislocation loop. This type of loop was also referred to as an R-dislocation by Kuhlmann-Wilsdorf (30).

The shear necessary to convert a sessile loop into a prismatic glissile loop can be imagined as taking place by the nucleation and sweeping of a Shockley partial loop over the area of stacking fault. Energetically, this process would be expected to occur readily

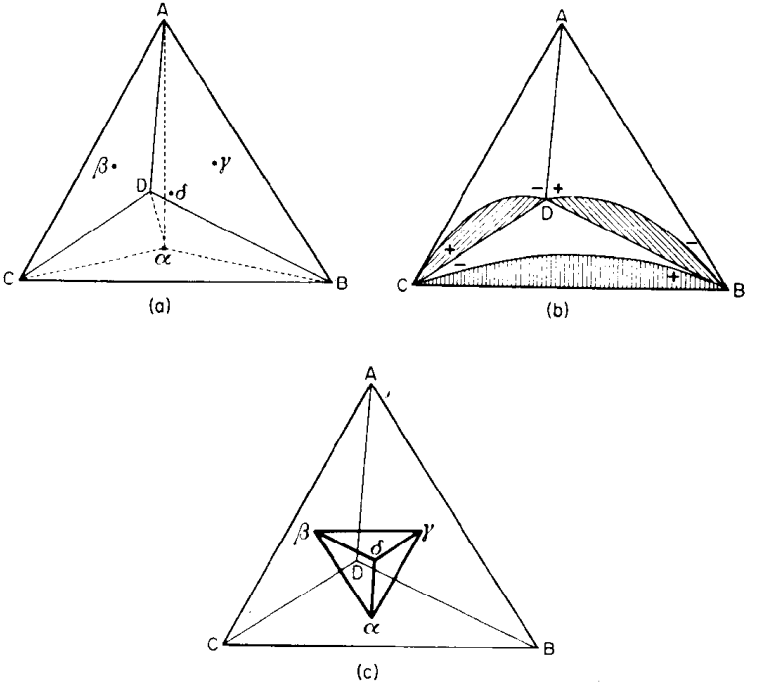

Fig. 2. (a) Thompson's reference tetrahedron *ABCD* with the midpoints of the faces labeled α, β, γ, δ; a Frank partial has a Burgers vector αA, a Shockley partial αB, αC, αD, etc., a low energy stair-rod $\alpha\delta$, $\alpha\beta$, $\alpha\gamma$, etc., and an unextended dislocation AD, AB, AC, etc. (b) The partials βA, γA, δA bowing out on the planes ACD, ADB, ABC, respectively; the relative signs of the dislocations near the nodes D, B, C are indicated. (c) The relationship between the defect tetrahedron $ABCD$ and the Burgers vector tetrahedron $\alpha\beta\gamma\delta$. (After Silcox and Hirsch (45), courtesy *Philosophical Magazine*)

in a metal of high stacking fault energy γ, where the increase in energy of the loop would be offset by the reduction in energy due to removal of the fault and where the nucleation of the sweeping partial might be aided by the surface tension of the fault. In metals of low stacking fault energy, the faulted sessile loop might be expected to be the stable form. According to Kuhlmann-Wilsdorf

(30), metals with $\gamma \sim 200$ ergs cm^{-2} are expected to contain prismatic loops, while metals with $\gamma \sim 20$ ergs cm^{-2} are expected to contain sessile loops. Thus, we might expect that quenched aluminum, a metal of high stacking fault energy, would contain prismatic whole dislocation loops, whereas quenched gold ($\gamma \sim 30$ ergs cm^{-2}) might contain faulted sessile loops. As will be seen below, gold contains stacking faults but not in the form of sessile

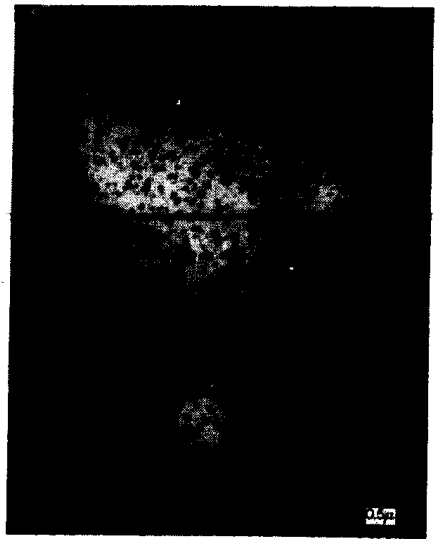

Fig. 3. Dislocation loops in aluminum quenched from ~600°C into iced brine. (After Hirsch *et al.* (35), courtesy *Philosophical Magazine*)

loops, while aluminum, although usually showing prismatic loops, may when very pure show faulted sessile loops. Thus, the simple stacking fault energy criterion for the conversion of sessile loops into prismatic loops is at present questionable, and it seems that certain other effects are also important.

B. DEFECTS IN QUENCHED ALUMINUM

Hirsch, Silcox, Smallman, and Westmacott (35) have examined thin aluminum foils (99.995% pure) prepared from thick (0.075 mm) specimens quenched from ~600°C into iced brine and aged at room temperature. Figures 3, 4, and 5 are typical electron micro-

graphs illustrating the dislocation loop distribution observed. There is no stacking fault contrast inside the loops, showing that they are prismatic loops. In Figure 3 the average diameter of the loops is $\sim$280 A, and the average loop density is $\sim 10^{15}$ cm^{-3}. The concentration of vacancies required to form the loops is $\sim 10^{-4}$. This is about the concentration of vacancies in equilibrium at high temperature (Bradshaw and Pearson (9)), and suggests that the formation of loops is the main mechanism for disappearance of

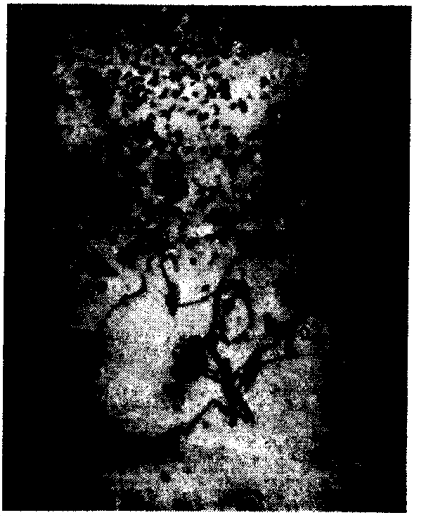

Fig. 4. Dislocation loops in aluminum quenched from $\sim$600°C into iced brine. Note that the density of loops is lower near the irregular dislocation lines. (After Hirsch *et al.* (35), courtesy *Philosophical Magazine*)

vacancies on aging at room temperature. The dislocation density in the loops is $\sim 10^{10}$ cm^{-2}.

Many of the loops are parallelogram-shaped (e.g., at *A* in Figs. 3, 4, and 5), others (e.g., at *B* in Figs. 3 and 5) appear as distorted hexagons, while the majority have an elongated shape as expected for a round loop viewed at an angle. Often a loop appears as two short arcs connected by less visible portions (e.g., at *C* in Fig. 5 and in Fig. 16 on page 24). This variation of image contrast around an inclined loop is expected on the kinematical theory of diffraction contrast (Hirsch, Howie, and Whelan (36)). Similar contrast effects have been observed at loops in zinc (Brown

(37), Price (38)) where the plane of the loop is parallel to the foil surface, and have been explained in detail by Howie and Whelan (39).

The plane of the dislocation loop is not easily identified from the image and diffraction evidence. However, Hirsch *et al.* (35) and Kuhlmann-Wilsdorf and Wilsdorf (40) have observed regular hexagonal loops, presumably lying on {111} planes with sides

Fig. 5. Aluminum quenched from ~600°C into iced brine. Note the denuded zone near the grain boundary. (After Hirsch *et al.* (35), courtesy *Philosophical Magazine*)

parallel to close-packed directions. These authors have also observed prismatic slip of such loops during examination. In view of the fact that prismatic slip occurs easily, it seems likely that many loops will have rotated from the {111} plane on which they were formed. Furthermore, the chemical stress due to the vacancy supersaturation when a {111} loop is growing would exert a couple on the loop tending to rotate it to a plane perpendicular to the glide cylinder, i.e., to a {110} plane. Thus many loops would be expected to be on {110} planes. On the other hand, if a hexagonal loop lies on {111} it can lower its energy by dissociation into

partials on the intersecting {111} planes. Kuhlmann-Wilsdorf and Wilsdorf (40) have examined the orientations of loops in quenched aluminum in some detail, and have put forward evidence that loops lie on {100}, {110}, and possibly on other planes as well as on {111}. Furthermore, they suggest that there is a tendency for loops of one orientation to form in one area, and that loops occur in groups with regions free of loops. They also found evidence for the occurrence of pairs of similar loops lying close together.

In many areas, irregular tangles of dislocations are observed (e.g., Fig. 4). These are presumably dislocations (possibly produced by quenching stresses) which have become heavily jogged by climb. The dislocation loop density is generally much smaller near these dislocations as expected if the dislocations act as preferential sinks for vacancies. Grain boundaries also act as sinks for vacancies and appear to hinder nucleation of loops in their vicinity. The denuded zone $\sim 1\mu$ wide near the grain boundary in Figure 5 is particularly striking.

All the observations so far described on quenched aluminum refer to 99.995% pure material (principal impurities Mg, Cu, Fe) and only whole dislocation loops were observed. Recently, Cotterill and Segall (41) have examined zone refined aluminum quenched from 600°C and have observed sessile hexagonal loops containing stacking faults. Figures 6 and 7 show typical examples. Similar contrast effects have been observed previously by Nicholson and Nutting (42) in aluminum + 16% silver alloys but not previously in aluminum. The loops are much larger than those in 99.995% pure material quenched from the same temperature and their density is much lower. In Figures 6 and 7 the loops are $\sim$2000–3000 A in size and their density is estimated to be $\sim 6 \times 10^{12}$ cm^{-3}. The vacancy concentration required to form the loops is again $\sim 10^{-4}$. The loops at *A* in Figure 6 are inclined at a large angle to the foil surface, and typical stacking fault interference fringes are visible. The fringes at *A* show the "reversal" effect explained in detail by Whelan and Hirsch (43). The loops at *B* in Figure 6 lie in a {111} plane nearly parallel to the foil surface ({112}); some of them, therefore, show widely spaced interference fringes. The hexagonal shapes of the loops are clearly evident. Figure 7a,b is a sequence of micrographs taken with a foil of (001) surface showing changes in the loops during observation. The foil

has been tilted during the sequence. Figure 7a is taken with a weak $(0\bar{2}0)$ reflection, while Figure 7b is taken with the same reflection, but close to the reflecting position (dynamical conditions of diffraction). The detailed interpretation of the contrast effects will not be discussed here. We note only that in Figure 7a most of the loops have faults, and that as judged by the contrast the loops are on various planes, e.g., *A* and *C* are on a different plane to *B* but

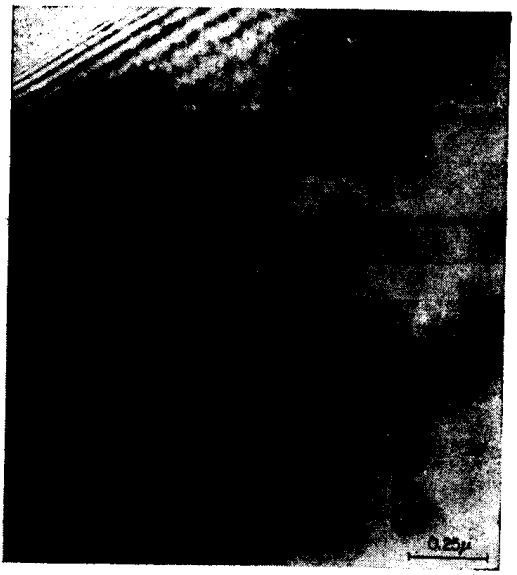

Fig. 6. Hexagonal sessile loops with stacking faults in zone refined aluminum quenched from ~600°C. *A:* Inclined stacking faults showing reversal of the contrast in interference fringes; *B:* sessile loops almost parallel to the surface. (After Cotterill and Segall (41))

appear similar in shape. In Figure 7b several sessile loops have been converted to prismatic loops of irregular shape, e.g., *A*, *B*, *C*, *D*, *E* (*B* and *D* are only faintly visible due to contrast conditions).

These observations by Cotterill and Segall clearly show that impurities have an important effect in determining the type of loop in quenched aluminum. A decrease in impurity content by a factor ~50 is sufficient to produce mainly faulted sessile loops. These results suggest that the type of loop produced by a quench (prismatic or sessile) is not governed only by the simple stacking fault energy criterion, but also seems to be sensitive to nucleating

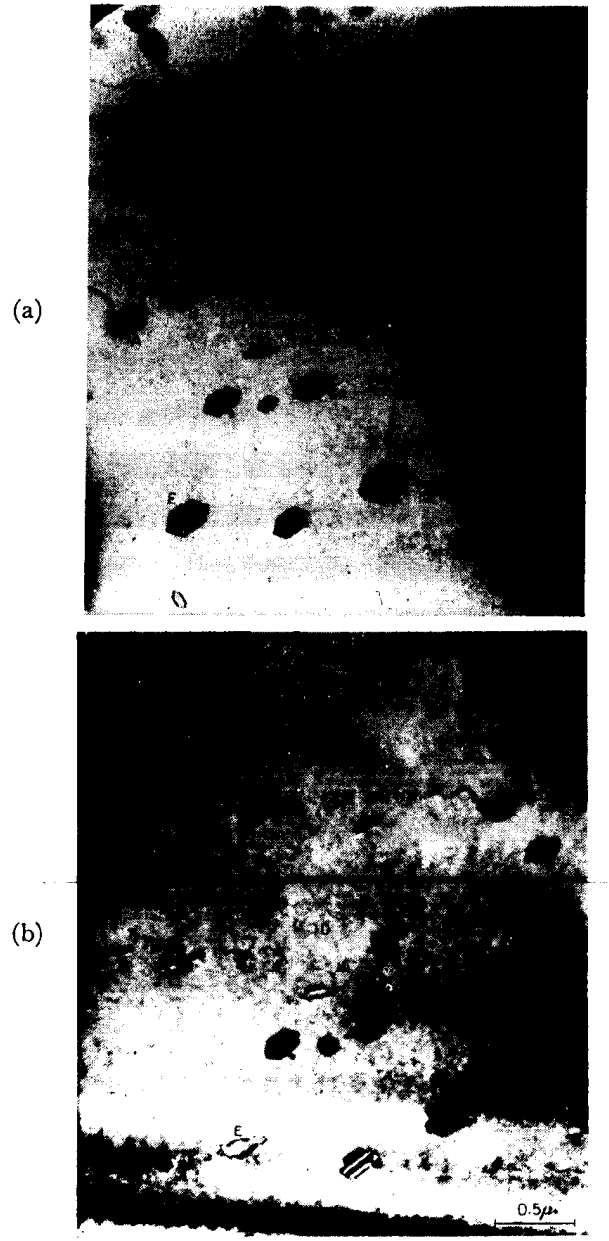

Fig. 7. Two micrographs of quenched zone refined aluminum showing changes in the loops. The sessile hexagonal loops A, B, C, D, E in (a) have been converted to prismatic loops in (b) during observation. (After Cotterill and Segall (41))

conditions. For example, the results can be understood qualitatively if nucleation occurs at impurities. A high density of nucleation sites seems to favor prismatic loops, while a lower density favors sessile loops. Cotterill and Segall (private communication) have also found that repeated quenching of 99.995% pure aluminum ultimately yields appreciable numbers of sessile loops. They interpret this result by suggesting that impurity atoms are swept out by interaction with migrating vacancies during the warm-up following a quench. If the impurities are trapped at the surface, for example, in the oxide film, repeated quenching will ultimately refine the material and give faulted loops. Cotterill and Segall find that four quenches from 600°C are sufficient to produce faulted loops in 99.995% pure aluminum. This interpretation, although tentative, is very attractive, and at the time of writing experiments are proceeding on this point.

C. DEFECTS IN QUENCHED GOLD

Quenching of gold has been studied by electrical resistivity measurements by Bauerle and Koehler (10); these workers found that for quenches from above 850°C a significant fraction ($\sim$10%) of the quenched in resistivity does not anneal out near room temperature. This result has been interpreted by Kimura, Maddin, and Kuhlmann-Wilsdorf (44) in terms of the formation of sessile loops containing stacking faults. Electron microscope experiments were therefore carried out by Silcox and Hirsch (45) to determine the nature of the quenching defects. The specimens (99.998% pure) were quenched into iced brine from temperatures between 910 and 960°C. They were aged for about one hour at temperatures between 100 and 250°C. Examination of the thinned foils revealed stacking faults, not in the form of discs as expected, but rather in the form of tetrahedra. Figures 8, 9, and 10 show typical examples of stacking fault tetrahedra viewed in different orientations ((100), (110), and (112), respectively). The average size of the tetrahedra for quenches from 910 to 960°C is $\sim$350 A and their density is about 5×10^{14} cm^{-3}. The average number of vacancies per tetrahedron is about 7400, and the corresponding total vacancy concentration is about 6×10^{-5}. Fringes associated with the stacking faults are clearly visible in Figure 10, as well as effects

associated with the truncation of the tetrahedra by the foil surfaces (Fig. 8 at *A*, Fig. 10 at *A*).

To understand the formation of a stacking fault tetrahedron, imagine a triangular sessile loop of Burgers vector αA occupying the area *CDB* of the {111} face of Thompson's tetrahedron in Figure

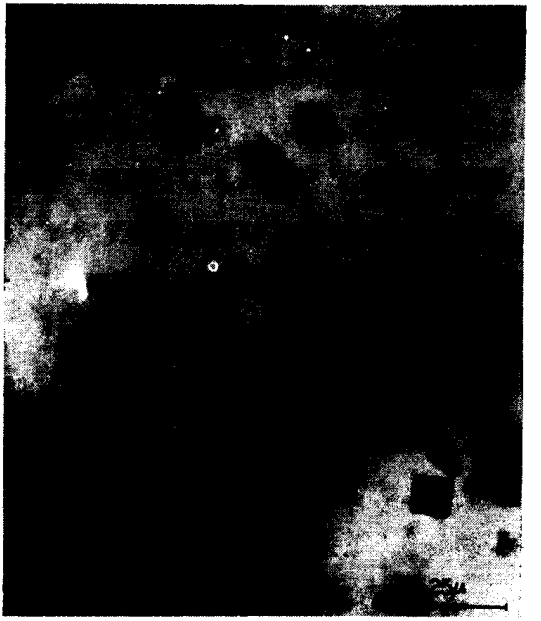

Fig. 8. Tetrahedra of stacking fault in quenched gold viewed along ⟨100⟩. Note that tetrahedron *A* is truncated by the surface. Quenching temperature ~960°C. (After Silcox and Hirsch (45), courtesy *Philosophical Magazine*)

2b. The Burgers vector αA of the sessiles along *CD*, *DB*, and *BC* may dissociate respectively according to the reactions

$$\alpha A \rightarrow \alpha\beta + \beta A$$
$$\alpha A \rightarrow \alpha\gamma + \gamma A$$
$$\alpha A \rightarrow \alpha\delta + \delta A$$

These reactions are energetically favorable since the Burgers vectors on the right include an angle of less than 90° and therefore repel each other by the Burgers vector squared criterion. $\alpha\beta$, $\alpha\gamma$, and $\alpha\delta$ are the Burgers vectors of sessile "stair-rod" dislocations (Thompson (33)) lying along *CD*, *DB*, and *BC*, while βA, γA, and